

M. SADHASIVAM<sup>1,3\*</sup>, M. USMANIYA<sup>2</sup>, L.J. BERCHMANS<sup>2</sup>, S.R. SANAKARANARAYANAN<sup>3</sup>,  
S.P. KUMARESH BABU<sup>3</sup>, G. VIJAYARAGAVAN<sup>1</sup>

## A LOW TEMPERATURE CALCIOTHERMIC REDUCTION APPROACH FOR THE SYNTHESIS OF LaB<sub>6</sub> POWDERS

In this work, we report the synthesis of a polycrystalline LaB<sub>6</sub> powders with a uniform morphology by a low-temperature metallothermic reduction route using calcium as a reductant. The processing methodology and heat treatment parameters are optimized based on thermodynamic estimates in order to favour the reaction kinetics and for complete formation of LaB<sub>6</sub> powders with highest purity. The synthesised powder was subjected to comprehensive characterization studies. X-Ray Diffraction (XRD) revealed the complete formation of LaB<sub>6</sub> compound without any traces of reactants. Scanning Electron Microscopy (FE-SEM) along with chemical mapping shows the morphology and elemental distribution of LaB<sub>6</sub> powder. X-Ray Photoelectron Spectroscopy (XPS) results show the futuristic peaks with photon energies that are assigned to the core levels of the La and B without significant impurities whereas the Fourier transform infrared (FTIR) spectrum indicates an apparent presence of La-B bonds at 1045.4 cm<sup>-1</sup>, 585.5 cm<sup>-1</sup>, and at 463.1 cm<sup>-1</sup>.

*Keywords:* LaB<sub>6</sub>; Metallothermic reduction; Characterization

### 1. Introduction

Rare earth-based hexaborides find wide spectrum of application because of their low work function, high emission density. In this family, Lanthanum hexaboride (LaB<sub>6</sub>) is an excellent thermionic electron emitter material with, brightness, chemical resistance, mechanical strength and low volatility. It also extensively finds application in electron microscopy as the source for electrons, spectroscopic techniques and in thin film coatings [1,2].

The common routes that are adopted for the synthesis of rare earth boride powders are solid-state reaction, sol-gel method, co-precipitation, arc/induction melting, hydrothermal process etc. But each of these conventional techniques has its own limitation as discussed elsewhere [3]. The synthesis of LaB<sub>6</sub> using the metallothermic reduction technique facilitates the process at the lower operating temperature coupled with superior powder yield. But even in the metallothermic reduction process, a careful exercise of process parameter optimization is required in order to achieve the chemical purity of the compound along with powder size and morphology. To end this, this research

has attempted to synthesise LaB<sub>6</sub> from La<sub>2</sub>O<sub>3</sub> and B<sub>2</sub>O<sub>3</sub> oxide precursors using Ca as a reductant. The heat treatment parameters are optimized based on the thermodynamic energy calculation of the involved chemical reaction and thus facilitating a complete synthesis of pure LaB<sub>6</sub> powders with defined morphology along with bulk yield.

### 2. Materials and methods

In the present study, the starting materials were reactant powders and reductant metal. Lanthanum oxide (La<sub>2</sub>O<sub>3</sub> – 99.9% Purity) purchased from Indian Rare Earth Ltd and Boron oxide (B<sub>2</sub>O<sub>3</sub> – 99.9% Purity) supplied by A.B. Enterprises, India, were used as reactant materials. Calcium metal (99% Purity) purchased from Loba Chemie, India, was used as the reductant. Metallothermic reduction route was adopted for the synthesis of Lanthanum hexaboride (LaB<sub>6</sub>). The steps involved in this synthesis are followed as reported in our earlier work [3] but with the optimized heat treatment parameters in order to achieve a complete reaction at the temperature of 900°C for 24 hours

<sup>1</sup> DEPARTMENT OF METALLURGICAL AND MATERIALS ENGINEERING, INDIAN INSTITUTE OF TECHNOLOGY MADRAS, CHENNAI – 600036, INDIA

<sup>2</sup> ELECTROPYRO METALLURGY DIVISION, CSIR-CECRI, KARAIKUDI-630003, INDIA

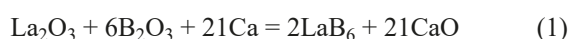
<sup>3</sup> DEPARTMENT OF METALLURGICAL AND MATERIALS ENGINEERING, NATIONAL INSTITUTE OF TECHNOLOGY TRICHY, TRICHY – 620015, INDIA

\* Corresponding author: [kgprad3@icrps.iitm.ac.in](mailto:kgprad3@icrps.iitm.ac.in)



under an inert argon atmosphere purged at a rate of 150 mL/min. The synthesized powder characteristics were studied with multiscale microstructural characterization. X-Ray Diffraction (XRD) was performed using (PANalytical) set up to analyze the formation of lanthanum boride phase and to identify the crystal structure. Differential scanning calorimetry (DSC, Setaram-Labsys Evo, France) measurement was carried out on the prepared  $\text{LaB}_6$  powders to understand its stability during heating up to  $1350^\circ\text{C}$  in the continuous flowing of high purity argon with heating rate of  $10^\circ\text{C}/\text{min}$ . To study morphology, particle size and microstructure of the obtained lanthanum boride Powder, field emission scanning electron microscopy [SUPRA-55VP, Zeiss] was carried out at an accelerating voltage of 25 kV. Energy dispersive spectroscopy (EDS) to detect chemical composition and elemental mapping. The chemistry of the powders along with the chemical and electronic state of the atoms are identified using X-Ray Photoelectron Spectrometer (XPS) [Multilab 2000]. The ionic vibrations and the stability of the synthesised powder were studied using the functional group Fourier transform infrared spectroscopy (FTIR) analysis [Perkin Elmer-Spectrum Two] between the wave number of  $4000$  to  $500\text{ cm}^{-1}$ .

The reaction for the synthesis of  $\text{LaB}_6$  can be expressed below,



Ca is chosen as reductant ahead of magnesium (Mg) since the Ellingham diagram with standard free energy demonstrates that calcium has the best tendency for oxide formation. In fact, it has the lowest free energy and is considered one of the best deoxidizing agents. The vapor pressure of calcium is adequately high, which permits a successful vapor stage calciothermic reduction of the reactants. The utilization of magnesium is likewise feasible because of its lower oxygen affinity. It is thermodynamically expected that the oxygen concentration under the Mg–MgO equilibrium will be higher than that of Ca–CaO. So, the calciothermic reduction of related oxides will be more favourable than magnesiothermic reduction. The secondary reason for choosing Ca as a reductant over Mg is the quantity of the used reductant.

In case of Mg, the quantity is always taken 15 to 20% in excess to the stoichiometric quantity in order to achieve a complete reaction. whereas in Ca, the reaction is more spontaneous, and the amount of reductant taken is the same amount as the stoichiometry of the reaction. According to the estimation of the Gibbs free energy, the overall reaction of Eq. (1) is thermodynamically spontaneous with a large negative free energy change of  $-3800\text{ kJ}$  at  $900^\circ\text{C}$  whereas the free energy change for Mg is  $-2900\text{ kJ}$  for the same temperature. Also, the enthalpy of mixing at this particular temperature is more exothermic for the reduction with Ca ( $-4400\text{ kJ}$ ) than Mg ( $-3820\text{ kJ}$ ) [4-6].

### 3. Results and discussions

The XRD results shown in Fig. 1(a) represent diffraction patterns corresponding to typical  $\text{LaB}_6$  Pm-3m space group cubic system indicating the successful formation of the crystals by the metallothermic reduction method. The presence of sharp and well-defined peaks, infers that the products were highly crystalline powders. The absence of any residuals viz.  $\text{La}_2\text{O}_3$  and  $\text{B}_2\text{O}_3$  suggests complete dissociation of reactants followed by optimized reductant addition and heat treatment parameters. DSC result in Fig. 1(b) indicates that  $\text{LaB}_6$  powders are stable and not decomposing into La and B during heating to  $1350^\circ\text{C}$  and thus corroborating the XRD results of complete formation of  $\text{LaB}_6$  product without any trace of intermetallic phase formation.

The FESEM image obtained along with the chemical mapping corresponding to the constituent elements of the  $\text{LaB}_6$  are shown in Fig. 2. The cubical morphology of the synthesised particles is observed in SEM image Fig. 2(a). The average particle size is in the range of  $18 \pm 2\ \mu\text{m}$  as shown in the Fig. 2(b). The elemental mapping corresponding to the region of Fig. 2(c) shows a homogeneous distribution La and B (Figs. 2e & 2f) without any discernible presence of impurities or reactant phases viz. O, C (not shown here). The elemental quantification indicates the complete crystallization of  $\text{LaB}_6$  powders as shown in Fig. 2(d).

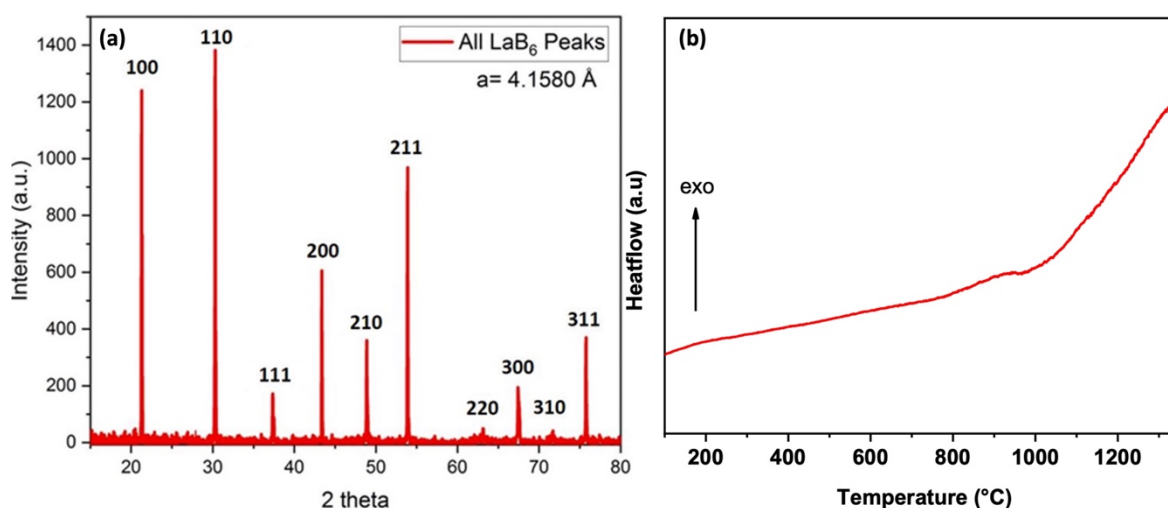


Fig. 1. (a) X-Ray Diffraction of  $\text{LaB}_6$  powders (b) Differential Scanning Calorimetry of  $\text{LaB}_6$

Fig. 3 displays the survey spectrum of the measured  $\text{LaB}_6$  at the photon energies of 1000-0 eV. As expected all the major futuristic peaks are assigned to the core levels of the La and B with the additional presence of C1s and O1s peaks, indicating some contamination of samples which may be originated from residual chamber contamination. The core level La 3d X-ray photoelectron spectroscopy (XPS) spectrum (Fig. 3(b)) with doublet spin orbiting splitting at 835.47 eV and 852.32 eV corresponds to  $\text{La}3d_{5/2}$  and  $\text{La}3d_{3/2}$ , respectively. While the interpretation of the core level La3d spectrum, the main peak attributed to the final states whereas the satellite peaks appeared at higher binding energies. However, this case is not suitable for all the transition metal-based compounds, In some cases; satellites are observed at lower binding energies too than the main

peaks. By means of assuming lowering the fermi energy level on the core-hole site of La 4f owing to its core-hole potential with empty states and filling the levels of La 3d orbitals. In accordance with this mechanism, there might be a possibility for two splits in configurations at their final states: hybridization of an electron near the fermi level populates and screens the potential of 4f level whereas on the other hand the same states (4f) remains to be empty and energy has been lowered down to its original fermi level. By considering the case of satellites peaks observed at lower binding energy compared to the main peaks, the sp bands of B1s orbital hybridized to the core-hole screening of final states of the main peaks in the photoemission process which may give rise to the shoulder (satellite peaks) for the La3d spectrum. In addition, the relative intensity of the two

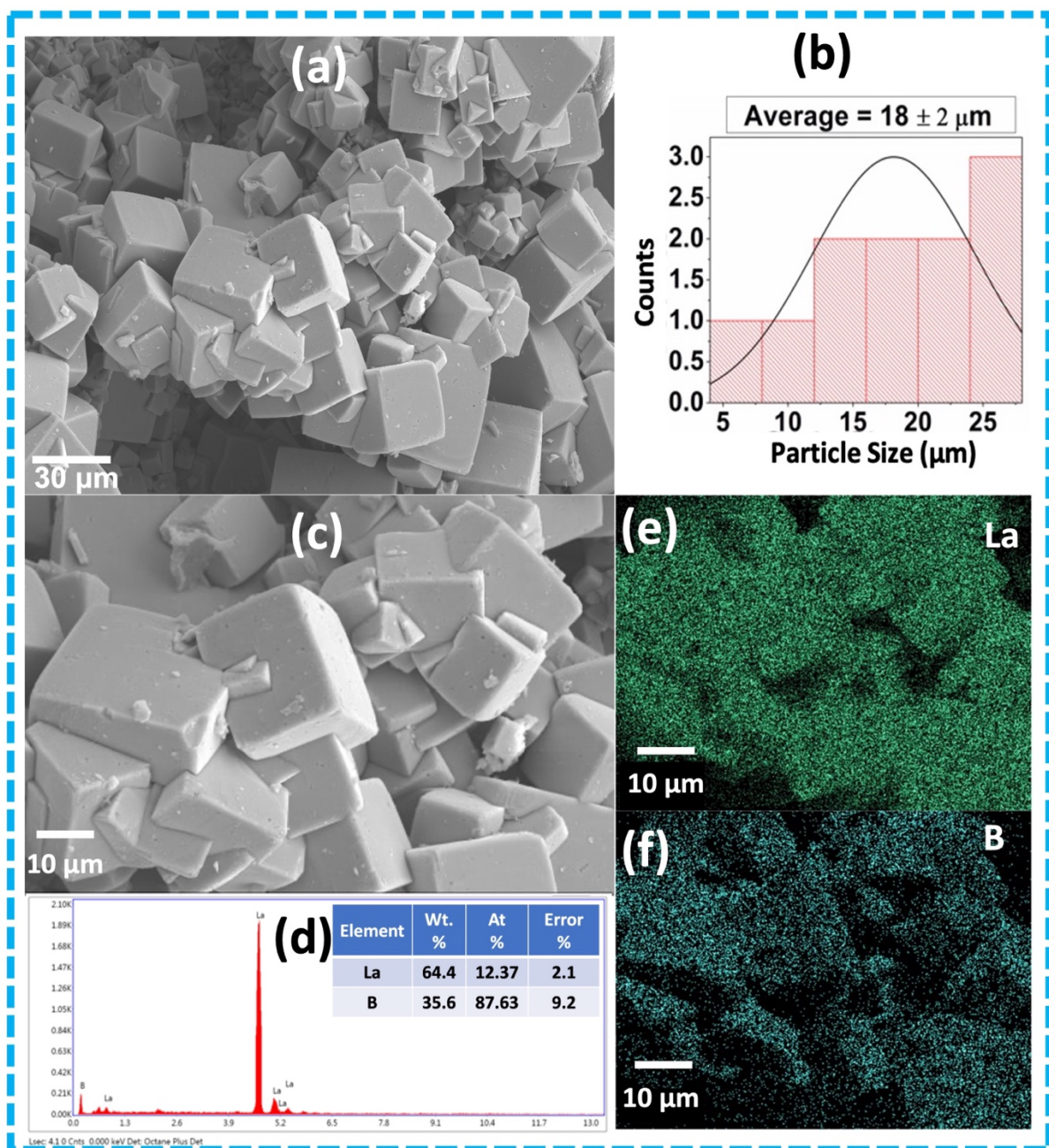


Fig. 2. (a) FE-SEM image of  $\text{LaB}_6$  particles (b) Particle size distribution, (c) SEM image corresponding to the area of EDS chemical mapping and spectrum (d) EDS spectrum along with quantification of  $\text{LaB}_6$  particle (e, f) Chemical mapping corresponding to La and B distribution respectively



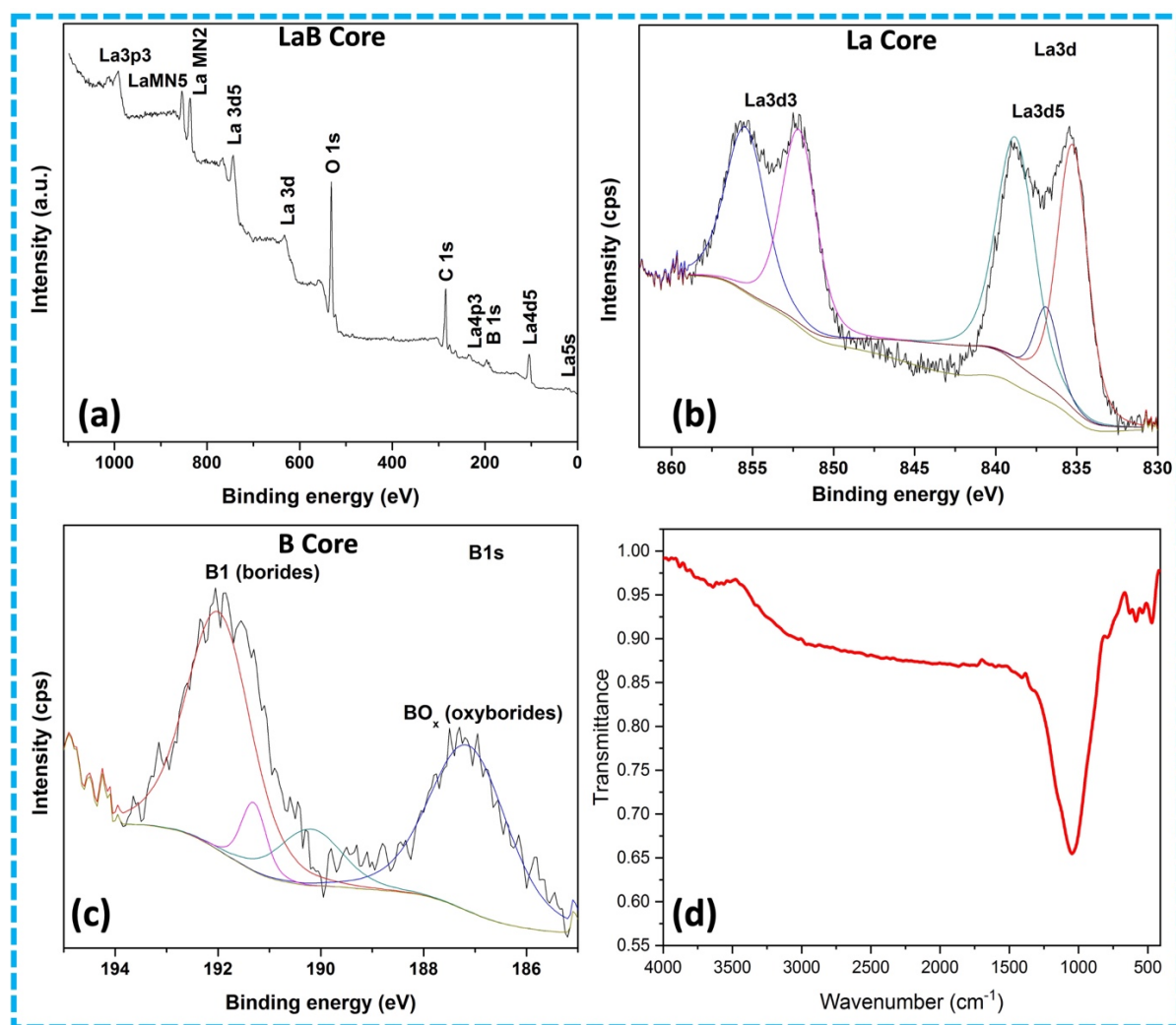


Fig. 3. XPS of (a) LaB core, (b) La Core, (c) B core, (d) FTIR of  $\text{LaB}_6$  powder

peaks (of La 3d) relies upon on the hybridization between the valence state of electrons and the La 4f states. For the case of pure lanthanum metal, the hybridization will be almost negligible due to the very small intensity of La3d peak screening. However, for the case of lanthanum boride ( $\text{LaB}_6$ ), there is existence of small hybridization but non-negligible existing between the B sp and La 4f orbitals. Consequently, clear and visible shoulder peaks existing for the La 3d in the XPS of  $\text{LaB}_6$ . Moreover, the doublet La3d spectrum with the separation of  $\sim 17$  eV between the peaks suggests the formation of non-oxidized lanthanum, which is in agreement with the existing literature [7,8].

Fourier transform infrared (FTIR) spectra of the  $\text{LaB}_6$  compound from (Fig. 3(d)) are recorded at 400 to  $4000\text{ cm}^{-1}$ . The FTIR spectra have shown some narrow and broad bands, with some shoulders. The existence of the prominent at  $1045.4\text{ cm}^{-1}$ ,  $585.5\text{ cm}^{-1}$ , and at  $463.1\text{ cm}^{-1}$  are responsible for the presence of La-B bond.  $3491.3\text{ cm}^{-1}$  O-H stretching and bending vibration of adsorbed water molecules.

The shown schematic in Fig. 4 explains the calciothermic reduction mechanism:

I.  $\text{La}_2\text{O}_3$  and  $\text{B}_2\text{O}_3$  reactants are thoroughly grounded and mixed in a mortar pestle.

- II. Ca metal is added as a reactant and the same has been packed in a sandwiched manner between reactants to facilitate better diffusion kinetics.
- III. Ca being the strongest reducing agent, reacts at  $900^\circ\text{C}$ .
- IV. The reactants are reduced and resulting in the formation of  $\text{LaB}_6$  along with the CaO as a by-product.
- V. 2M HCl acid leaching was carried out to neutralize the CaO by-product which results in the formation of  $\text{CaCl}_2$  salt and  $\text{H}_2\text{O}$ .
- VI. The salts and water are evaporated by heating the product at  $200^\circ\text{C}$  for 30 min to obtain pure  $\text{LaB}_6$  powders.

#### 4. Conclusions

In the present research synthesis of lanthanum boride ( $\text{LaB}_6$ ) was synthesized using low-temperature metallothermic reduction method with optimized processing and heat treatment parameters. Below are the observation based on the characterization studies,

1. XRD results indicate the complete formation of  $\text{LaB}_6$  without any residual reactant.



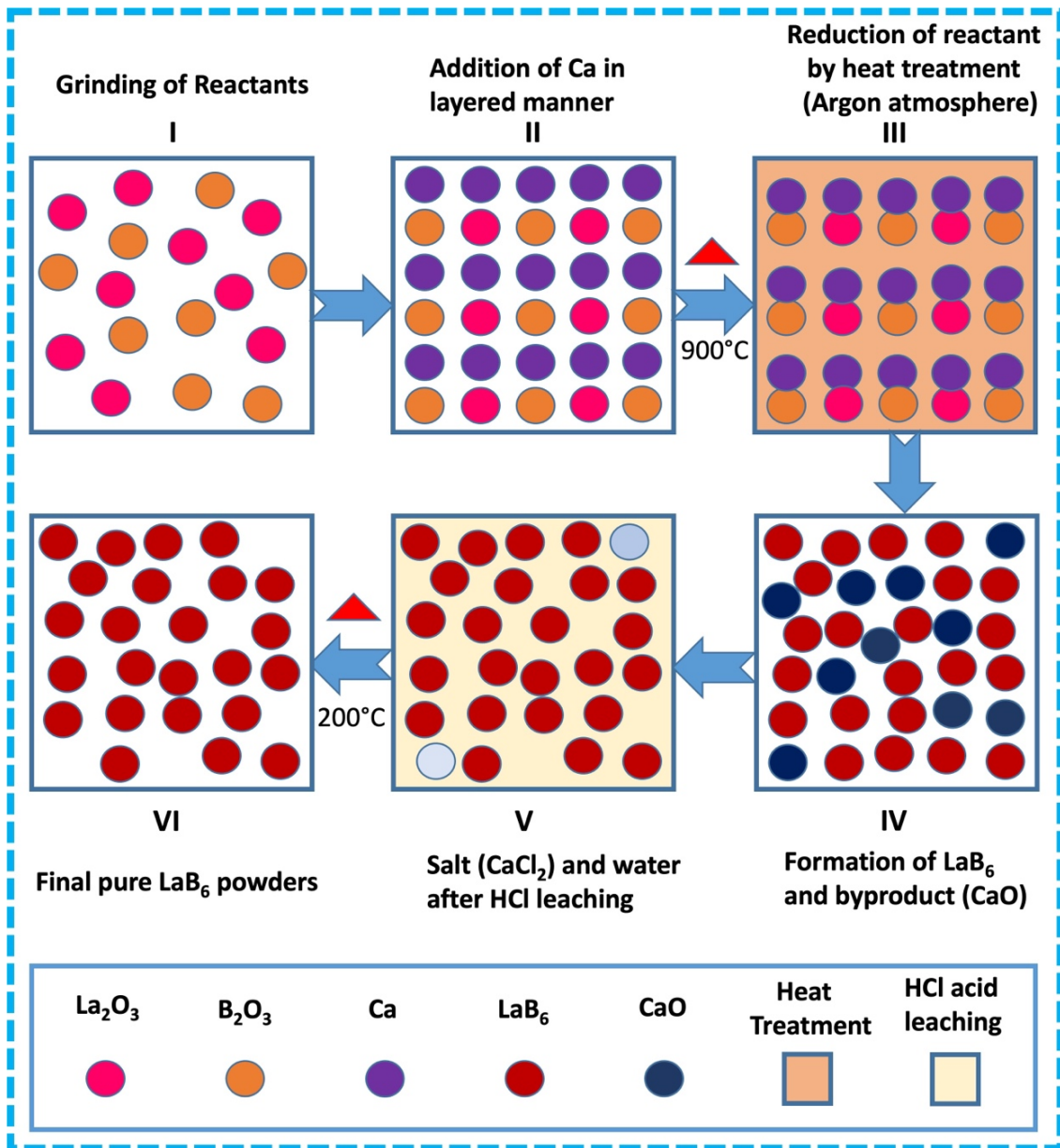


Fig. 4. The mechanism involved in the synthesis  $\text{LaB}_6$

- FE-SEM along with chemical mapping shows the formation of  $\sim 20$  micron-sized cuboidal morphology  $\text{LaB}_6$  powder
  - X-Ray Photoelectron Spectroscopy (XPS) results shows the futuristic peaks with photon energies that are assigned to the core levels of the La and B without significant impurities
  - Fourier transform infrared (FTIR) spectrum indicates an apparent presence of La-B bonds at  $1045.4\text{ cm}^{-1}$ ,  $585.5\text{ cm}^{-1}$ , and at  $463.1\text{ cm}^{-1}$
- REFERENCES
- J.A. Zaykoski, M.M. Opeka, L.H. Smith, I.G. Talmy, J. Am. Ceram. Soc. **94** (11), 4059-4065 (2011).
  - R.K. Selvan, I. Genish, I. Perelshtein, J.M. Moreno, J. Gedanken, Phys. Chem. C **112**, 1795-1802 (2008).
  - M. Sadhasivam, L.J. Berchmans, G.K. Meenashisundaram, U. Mehana Usmaniya, S.R. Sankaranarayanan, S.P. Kumares Babu, J. Min. Metall. Sect. B-Metall. **56** (1), 77-87 (2020).
  - B. Bertheville, J.E. Bidaux, J. Alloy. Compd. **387**, 211-216 (2005).
  - Tuncay Simsek, Arun K. Chattopadhyay, Mustafa Baris, Murat Bilen, Journal of Solid-State Chemistry **276**, 238-243 (2019).
  - M. Zhang, X. Wang, X. Zhang, P. Wang, S. Xiong, L. Shi, Y. Qian, J. Solid State Chem. **182**, 3098-3104 (2009).
  - Kotani, M. Okada, T. Jo, A. Bianconi, A. Marcelli, J.C. Parlebas, J. Phys. Soc. Jpn. **56**, 98 (1987).
  - L. Perkins, M. Trenary, T. Tanaka, S. Otani, Surf. Sci. **423**, 1, L222-L228 (1999).